

**SAE TECHNICAL
PAPER SERIES**

1999-01-0524

Investigation of Cavitation in a Vertical Multi-Hole Injector

C. Arcoumanis, H. Flora, M. Gavaises and N. Kampanis
Imperial College of Science, Technology and Medicine

R. Horrocks
Ford Motor Co.

**Reprinted From: Technology for Diesel Fuel Injection and Sprays
(SP-1415)**



**International Congress and Exposition
Detroit, Michigan
March 1-4, 1999**

The appearance of the ISSN code at the bottom of this page indicates SAE's consent that copies of the paper may be made for personal or internal use of specific clients. This consent is given on the condition however, that the copier pay a \$7.00 per article copy fee through the Copyright Clearance Center, Inc. Operations Center, 222 Rosewood Drive, Danvers, MA 01923 for copying beyond that permitted by Sections 107 or 108 of the U.S. Copyright Law. This consent does not extend to other kinds of copying such as copying for general distribution, for advertising or promotional purposes, for creating new collective works, or for resale.

SAE routinely stocks printed papers for a period of three years following date of publication. Direct your orders to SAE Customer Sales and Satisfaction Department.

Quantity reprint rates can be obtained from the Customer Sales and Satisfaction Department.

To request permission to reprint a technical paper or permission to use copyrighted SAE publications in other works, contact the SAE Publications Group.



No part of this publication may be reproduced in any form, in an electronic retrieval system or otherwise, without the prior written permission of the publisher.

ISSN 0148-7191

Copyright ©1999 Society of Automotive Engineers, Inc.

Positions and opinions advanced in this paper are those of the author(s) and not necessarily those of SAE. The author is solely responsible for the content of the paper. A process is available by which discussions will be printed with the paper if it is published in SAE Transactions. For permission to publish this paper in full or in part, contact the SAE Publications Group.

Persons wishing to submit papers to be considered for presentation or publication through SAE should send the manuscript or a 300 word abstract of a proposed manuscript to: Secretary, Engineering Meetings Board, SAE.

1999-01-0524

Investigation of Cavitation in a Vertical Multi-Hole Injector

C. Arcoumanis, H. Flora, M. Gavaises and N. Kampanis
Imperial College of Science, Technology and Medicine

R. Horrocks
Ford Motor Co.

Copyright © 1999 Society of Automotive Engineers, Inc.

ABSTRACT

An enlarged transparent model of a six-hole vertical diesel injector has been used to allow visualization of the flow at Reynolds and cavitation numbers matching those of real size injectors operating under normal Diesel engine conditions. The visualization system comprised a CCD camera, high-magnification lenses and a spark light source which allowed high-resolution images to be obtained. The flow conditions examined in terms of flow rates and pressures covered the range from low to full load of the real size injector while the needle lift position corresponded to that of full lift of the first- and second- stage in two-stage injectors. In addition, different values of needle eccentricity were tested in order to examine its effect on the cavitation structures within the injection holes.

From this investigation two different types of cavitation were identified: cavitation originating at the entrance to the injection holes and cavitation strings formed inside the sac volume and linking adjacent holes. In the former case, the flow pattern mainly depended on the cavitation rather than the Reynolds number as well as on the needle eccentricity. Different types of cavitation structure were identified varying from incipient bubbly flow to plug-type cavitation films and fully separated flow. In addition to hole cavitation, cavitation strings were found to form transiently inside the sac volume. As these cavitation strings were convected by the mean flow towards the injection holes, they were interacting transiently with the pre-existing cavitation structures resulting in a rather chaotic hole flow pattern. Since this phenomenon was found not to occur simultaneously in all injection holes, transient differences in the flow exiting the different injection holes were observed.

Overall, the results revealed that the flow development in multi-hole vertical nozzles, despite the axisymmetric geometry, may lead to hole-to-hole flow variations as a result of the transient nature of the cavitating structures formed inside the sac volume and holes.

INTRODUCTION

Over the last few years numerous studies have revealed that the fuel injection system of direct-injection Diesel engines

plays the dominant role on the spray development and pollutant formation mechanisms. The demand for well atomized fuel sprays has led to an increase of the injection pressure up to 1500 bar and beyond, to the design of electronic systems which can accurately control the injection period and injection quantity and to the manufacturing of nozzles with an increased number of smaller holes which can distribute the fuel more uniformly in the piston bowl. Recently, common-rail injection systems have been developed [1,2] which allow fuel injection under high and relatively constant pressure independent of the pump/engine speed.

Irrespective of the mechanism that generates the high pressure itself, inclined injectors have been used in 2-valve DI Diesel engines, while vertical injectors have recently been introduced in 4-valve engines. Although the flow distribution in these two different nozzle configurations varies considerably, hole cavitation seems to be a common feature of their hole flow. This phenomenon has been previously identified to occur at the hole inlet due to the sudden local pressure drop occurring at the recirculation zones formed in these areas; it is more prominent at higher injection pressures and smaller hole sizes and becomes unavoidable in advanced fuel injection systems independent of the back pressure. Since the cavitating structures exiting from the injection holes have been identified to have a profound effect on the atomization process of the diesel spray, for example see [3-10], a number of recent investigations have focused into this area. Special emphasis has been given to the visualization of the flow itself as well as to its link with the spray characteristics. Since optical access to real-size multi-hole nozzles operating under real injection pressures cannot easily be obtained, large scale models [11-19] or single-hole axisymmetric configurations of real-size nozzles [20-25] have been used instead in order to provide indirect evidence of the flow structure under similar operating conditions.

Despite its importance, research into nozzle cavitation is incomplete and inconclusive; the next section of the paper reviews previously published studies in order to highlight the most important conclusions as well as topics that require further investigation. Furthermore, basic phenomena taking place in cavitating flows, such as nucleation, bubble dynamics and flow transition are also reviewed in order to assist the interpretation of the results.

The experimental system used in the present investigation is then presented together with the operating conditions tested; it comprises a fully transparent large scale model of a vertical six-hole conical sac-type nozzle incorporated into a steady flow rig. Emphasis has been given to the simultaneous matching of both the Reynolds and cavitation numbers, which allows proper correlation of the two-phase flow characteristics between the enlarged and real size nozzles. The results obtained during the present work are then presented and discussed followed by the most important conclusions.

NOZZLE FLOW UNDER CAVITATING CONDITIONS

This section describes the main findings from studies that have been reported in the open literature using transparent nozzles with emphasis given to the characterization of the cavitation phenomena.

Large scale models

Since real size nozzles have very small dimensions and operate under very high pressures over very short times, most of the studies up to now have been performed on large scale models operating under steady-state conditions; dynamic flow similarity has been generally employed in order to correlate the flow characteristics with those of real size nozzles. Table 1 summarizes these studies together with the main parameters that have been matched in the dynamic flow similarity. As can be seen, in most studies the Reynolds number is kept similar to that of real size nozzles, and in some cases the refractive index of the liquid has been adjusted to be identical to that of the acrylic nozzle wall in order to allow laser Doppler velocimetry (LDV) measurements of the internal liquid flow. Similarity based on matching both the cavitation and Reynolds numbers simultaneously has also been achieved in references [18,20]. However, as it will be further explained in the following section, the behavior of the cavitation bubbles depends not only on the cavitation number but also on the actual pressure surrounding them. An additional complication arises from the fact that liquids can theoretically withstand tension of the order of a few hundred bars before the formation of vapor (for a detailed review see [26]). Real liquids (both single- and multi-component) start to boil in a much higher pressure, that is usually referred to as the vapor pressure, due to the presence of nuclei in the fluid. Since the nuclei size distribution in liquids varies, this can lead to a different threshold pressure for cavitation even if the cavitation number is kept the same [27]. Irrespective of the above difficulties in establishing the link between the flow characteristics of large scale and real-size nozzles, some important features have been identified in large scale nozzles which can be summarized as follows:

- the flow in the injection hole prior to cavitation is turbulent [4,12,17] with an increasing intensity after the onset of cavitation [20]. The needle lift modifies the local flow field at the entrance to the holes with more distinguishable differences present in VCO nozzles.
- cavitation initiates in areas of local pressure minimum which depend on the specific nozzle design and the

actual position of the needle [5,12,14]; the most frequent case is the top corner of the injection holes.

- important differences in the type of two-phase cavitating flow have been identified for different combinations of Reynolds and cavitation numbers [20]. Although many studies have focused on establishing the transition criteria for the various two-phase flow regimes, for example see [28], these can not be directly applied to the cavitation in diesel injectors due to the very short residence time of the bubbles in the injection holes. Certainly, this is more true in real-size nozzles where flow velocities are much higher.
- despite the difficulties in extrapolating the results from large scale nozzles to real-size ones, it is expected that, for Reynolds and cavitation numbers of practical interest, small bubbles or opaque foam are formed and, in some cases, plug-type flow together with larger bubbles [20]
- the enhanced hole turbulence in the presence of cavitation has been found to be an important parameter in liquid jet atomization [3]
- similarities have been observed in the structure of sprays generated by large scale and real-size nozzles operating under similar cavitation and Reynolds numbers [18].

Overall, it should be noted that although a number of experimental studies have investigated the size distribution of bubbles in bubbly flows [29,30], these studies have focused more on the basic characteristics of the motion of pre-existing bubbles rather than on the understanding of the two-phase bubbly flow present in diesel injection nozzles.

Real-size nozzles

Studies that have been performed in real size but simplified hole geometries are also very important since they refer to dimensions and pressures similar to those of production nozzles; Table 2 summarizes them. Unfortunately, such studies have been performed in less practical geometries such as in single-hole axisymmetric nozzles [20-25], although transient conditions in the hole have been achieved [21,25]. Since the size of the injection hole is very small, most of the obtained images have low resolution and are inadequate to resolve the details of the cavitation structures. Some earlier studies [31-33] have focused on the effect of hole cavitation on the discharge coefficient of the injection hole and also on its influence on the spray characteristics [5-7]. The following conclusions seem to be common in most investigations obtained in real-size single-hole nozzles:

- hole discharge coefficient decreases with increasing cavitation number
- hole inlet geometry (radius of curvature) greatly affects the spray characteristics and the hole discharge coefficient
- the spray cone angle increases and the droplet SMD decreases with increasing cavitation number; however, the effect on the droplet size can be also attributed to the higher droplet velocities and Weber number effects associated with the higher injection pressures
- hole cavitation seems to cover the whole entrance region and it is usually extended up to the exit of the injection hole [21-25]. However, it is not clear whether the structures consist of individual bubbles or slug flow

- in the presence of cavitation the liquid injection velocity increases due to the void inside the injection holes [8,23-24] which gives a smaller effective exit hole area

In general, many studies [4-10,14,18,21-25,31] have demonstrated that the presence of either cavitation bubbles or dissolved gas in the liquid fuel have a strong effect on the atomization process, thus necessitating a more detailed investigation of the onset and development of the cavitation structures within the nozzle.

In addition to the experimental studies on cavitation in Diesel nozzles, various fundamental physical processes taking place during the onset and development of cavitation have been investigated independently and require special attention. These are mainly related to phase transition and bubble dynamics phenomena and are briefly summarized in the following section.

Phase transition & bubble dynamics

This section examines various characteristics of the phenomena related to bubble dynamics, which can be used in order to understand the initiation and further development of hole cavitation. By considering the similarities between cavitation and the boiling process, many characteristics of the boiling flows that have been extensively investigated in the past can be applied to diesel nozzles. Areas of interest include those related to the formation of bubbles either from the bulk of the liquid or from heated/unheated walls, their further growth and convection inside the injection hole and the possible formation of another two-phase flow regime (i.e. slug or annular flow) as the void fraction of the vapor phase increases.

Although theoretical and experimental studies on the pressure-temperature level required to induce a phase transition from liquid to vapor have revealed that liquids can withstand tension [26], in most applications two general cases typically occur: first, the thermal motion within the liquid may form temporary microscopic voids that can constitute the nuclei necessary for rupture and formation of macroscopic bubbles; this is known as homogeneous nucleation. On the other hand, in systems where a solid boundary does exist, the solid walls depending on their surface roughness may act as a reservoir of microscopic particles suspended in the liquid; in this case bubble formation starts from points near the wall and it is called heterogeneous nucleation. Many investigations have been concerned with a detailed description of this type of process and extensive reviews can be found in [34-38]. What complicates matters is that the initial number (per unit volume) of the nuclei and their size distribution is unknown and rather difficult to be estimated in a liquid since this depends on the chemical composition of the fuel and on the flow conditions. Some relevant studies have been reported in [37,39-43] but it is still unclear what is the nuclei size distribution in hydrocarbon fluids such as the diesel fuel. The degree of the dissolved gas is another important factor having an effect on the nuclei distribution since a higher percentage of dissolved gas leads to an increase in nuclei population number and size [38].

At this point additional considerations should be given to the effect on cavitation of the presence of solid walls, the wall

surface roughness and its temperature which are important parameters in production nozzles installed in an engine cylinder head, since a number of studies have demonstrated (for example [44-48]), that heterogeneous nucleation is more pronounced than the homogeneous case. This phenomenon is greatly affected by the wall roughness (rough walls increase the population of active nuclei sites), the interaction of the working fluid with the wall material (which alters the adhesion forces acting on the bubbles formed on the walls) and the dynamics of the bubble growth along the walls. Furthermore, the interaction of the bubbles growing on the wall with the boundary layer is a subject that requires special attention. Wall temperature has also a profound effect on the nucleation process since a higher wall temperature increases significantly the number of active nucleation sites. Thus, the 3-D temperature distribution on the nozzle walls should be known for a detailed approach, which necessitates a heat transfer investigation within the injector body as a function of the flow conditions inside the nozzle holes. Heat transfer studies in boiling two-phase flow systems have been performed in the past (established theories can be found in [36-38,48]), but such an investigation in real nozzles has not been performed up to date. Overall, out of these processes one should be able to determine the bubble size distribution as well as the frequency of their detachment from the wall. These bubbles together with those resulting from the homogeneous nucleation process act as initial sites for further bubble growth during their travel through the liquid.

Summarizing, it can be argued that in large-scale transparent models homogeneous nucleation is responsible for the onset of cavitation, while in real-size nozzles installed in engines the heterogeneous case should prevail; thus, differences are expected to exist in the onset and development of cavitation between real and large scale nozzles. Unfortunately, characterization of these differences hasn't been possible yet.

Following their formation, investigation of the dynamics of individual spherical bubbles becomes important. Existing theories employ the momentum equation for the estimation of the net forces acting on the liquid interface. Further complications include viscous, compressibility, mass diffusion and heat transfer effects; typical investigations are those reported in [49-53] and extensive reviews are given in [27, 35, 54]. Further developments are those concerned with nonlinear effects [55], non-equilibrium effects [56], interaction of bubbles with free surfaces [57] as well as the dynamics of the interactions between bubbles [58-60]. These models predict the dynamic variation of the bubble volume as it moves in a transient pressure field and account for the evaporation of the liquid phase as well as for the dynamics of bubbles containing both dissolved gas and liquid vapor. Relatively few studies have focused on the motion of bubbles and relevant theories are summarized in [61-63]. These studies report correlations for the drag coefficient of moving bubbles as well as estimates of the forces acting on them, required for the calculation of their movement. Areas for further investigation include the interaction of bubbles with the liquid turbulence as well as the motion of clouds of bubbles where possible collisions would significantly modify their dynamic behavior. It is also possible

that the presence of walls and the bubble density could influence the sphericity of bubbles during their motion.

An area of further research is related to the evaporation process of the multi-component diesel fuel. In the boiling of multi-component mixtures, the heat and mass transfer processes are closely linked to the evaporation rate, which is greatly affected by the difference in the boiling point of the various components. This is significantly different from single-component systems where interfacial mass transfer rates are normally very high. Although some studies have been reported on these issues as well as on the nucleation process of a multi-component mixture, it is generally accepted that a number of uncertainties still exist which limit the ability to model the bubble dynamics; a comprehensive review of these issues is given in [64].

From the analysis of the above studies it is evident that the growth rate of individual bubbles depends on the actual pressure around them rather than on the dimensionless cavitation number. This represents an additional complication in extrapolating the conclusions from large-scale transparent nozzle investigations to real-size production nozzles.

Another area of interest is related to the classification of the various types of two-phase flow and the transition criteria from one flow type to the other. Since there are many types of two-phase flows which can be distinguished from differences in the spatial distribution of the surface interface between the vapor and the liquid phases (topology), it has not been possible up to now to develop a single model that describes all cases; only empirical correlations can be used as criteria for distinguishing between the flow regimes which also depend on the specific application. As a result, depending on the flow topology, models exist for the particulate, bubbly, slug, annular or other flow types; reviews on the differences between these two-phase flow regimes can be found in [65]. Nevertheless, these flow regimes may co-exist in hole cavitation which complicates relevant analytical investigations. Despite these difficulties, one simple and easily applied criterion for flow transition is based on the local void fraction of the vapor or gaseous phase; if this is less than 30% then the bubbly flow regime seems to prevail, which also depends on the velocity of the fluid and the time available to become fully mixed. As the velocity of the fluid increases, the void fraction required for transition from bubbly to slug flow increases and values up to 60% have been reported. It seems that for larger vapor volume fractions, the flow becomes misty and depending on the specific geometry and the local pressure and temperature, a fully separated or fully mixed flow is more likely to occur.

Having analyzed the findings from previous studies on nozzle cavitation and the physical parameters that affect its formation and further development, we can now proceed to the description of the experimental system used in the present investigation and the presentation of the results obtained in the transparent large-scale multi-hole nozzle.

EXPERIMENTAL SYSTEM

The experimental rig, shown in Figure 1, is very similar to that previously reported in [12]. The flow rate is continuous and constant while the working fluid has the same refractive

index to that of the transparent material; as a result, the illumination light can penetrate through the liquid-solid interfaces without distortion which allows for flow visualization or LDV measurements. The working fluid is a mixture of 31.8% by volume of 1,2,3,4-tetrahydronaphthalene (tetraline) and 68.2% oil of turpentine with a density and kinematic viscosity of 0.893 kg/m^3 and $1.64 \times 10^{-6} \text{ m}^2/\text{s}$ at 25°C . The mixture was maintained at a temperature of $25 \pm 0.2^\circ\text{C}$ by a temperature controller, using a heater and a cooler installed within the storage tank and a platinum resistance sensor near the pump outlet, to maintain the fluid refractive index at a level of 1.49 which is identical to that of the cast acrylic. The flow rate of the mixture was controlled by a valve in the pipe downstream of the pump and measured by an orifice plate, calibrated to be accurate within 3%. The properties of this particular fluid mixture are comparable to that of light diesel fuel. In order to match both the Reynolds and the cavitation numbers, a suction pump was added downstream of the transparent model in order to create sub-atmospheric pressures at the nozzle exit; the pressure at the exit of each injection hole was monitored with a manometer.

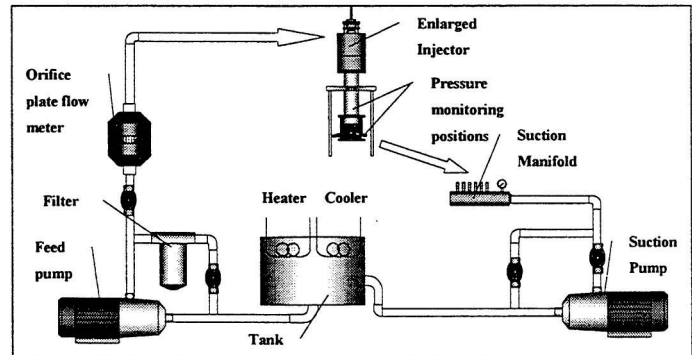


Figure 1 - Schematic representation of the experimental rig

The dimensions of the nozzle and the needle represent a 20x magnification of a Bosch six-hole vertical diesel injection nozzle; the nominal hole size of the model is 3.52 mm which corresponds to a hole size of 0.176 mm in the real injector with sharp inlet edges. The geometry of the large-scale model corresponds to a conical mini-sac type vertical nozzle and the details can be found in [12]. The needle stop positions of the first and second stage were 0.08 and 0.3 mm, respectively, which correspond to 6.0 and 1.75 mm, respectively in the large scale model. Images were obtained for different needle positions within the above limits for a variety of Reynolds and cavitation numbers¹, which are listed in Table 3. By employing dynamic flow similarity, the operating values of the real size nozzle can be estimated; these are also listed in Table 3. On the basis of the Reynolds number similarity it can be concluded that the flow rates investigated here correspond to those of low to full load, while from the cavitation number similarity it can be deduced that the corresponding injection pressure of a real

¹ The Cavitation Number is here defined as: $\text{CN} = \frac{P_{\text{inj}} - P_b}{P_b - P_v}$ where P_{inj} is the injection pressure, P_b is the back and P_v is the vapour pressure.

size nozzle can be as high as 800 bars assuming a typical back pressure at the time of the start of injection of 40 bars.

In order to visualize the flow inside the injection holes after the onset of cavitation, a CCD camera (Sensicam) was used, with illumination of the test area provided by either a laser or a spark light (see Figure 2). Good illumination of the testing area was one of the key parameters for obtaining clear images.

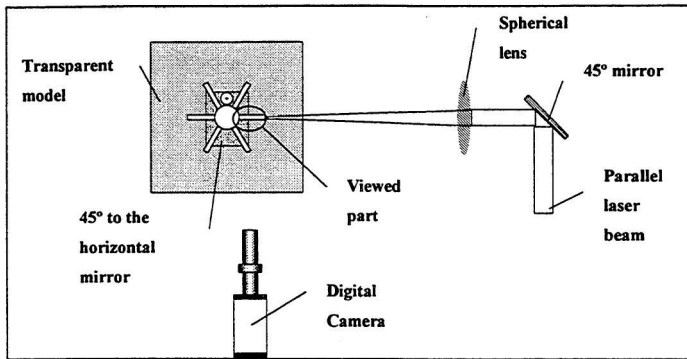


Figure 2 - Light and camera orientation (Plan view)

The Sensicam system is a high-resolution fast-shutter unintensified CCD camera. The resolution of its sensor is 1280 x 1024 pixels at a sensitivity of 12 bit. The sensor was Peltier cooled to -15°C for increased sensitivity and low noise operation. The shutter speed could be adjusted between 100 μs to 1ms with a freely programmable multiple exposure capability allowing up to 10 shots to be included in a frame. Since one of the main aims of the investigation is to identify different flow structures within the injection hole, high magnification lenses were used. The focal area with the best possible magnification obtained in the present investigation was covering approximately 1/3 of the hole width which allowed for details of the flow structures to be clearly resolved within the injection hole.

RESULTS AND DISCUSSION

In this section the various results obtained are described including the monitoring of the flow conditions at which cavitation initiates and disappears, the variation of the nozzle discharge coefficient as a function of the cavitation number, and the cavitation development under different flow conditions and needle positions.

Cavitation onset

The first phenomenon examined was the monitoring of the flow conditions at the onset of hole cavitation as a function of the Reynolds and cavitation numbers for different needle lifts. Figure 3 shows the cavitation number at which cavitation bubbles were becoming visible as a function of the Reynolds number for the needle positioned at its full lift, while Figure 4 shows again the onset cavitation number for different needle lifts. It is immediately apparent that the onset of cavitation occurs at almost the same cavitation number independent of needle lift. It is well known [12] that, for different Reynolds numbers (corresponding to different flow rates) and needle lift

positions, the local pressure minimum occurring at the entrance to the injection hole where cavitation initiates, varies considerably in strength and spatial distribution. That implies that the threshold pressure for cavitation is not the constant vapor pressure of the liquid, as it is usually assumed, but it depends on the detailed nuclei distribution of the flowing liquid. This statement is verified in Figure 5 which demonstrates the hysteresis identified on the cavitation number at which cavitation bubbles were disappearing relative to that at the onset of cavitation. As it is clear, for the same flow rate and needle lift position, cavitation seems to be suppressed at lower values of the cavitation number implying that the cavitation bubbles themselves act as nuclei, in addition to the other sources such as particles, dissolved gas and wall nuclei that exist within the flowing liquid itself; hence, less tension is needed to sustain cavitation. The above analysis confirms that the liquid composition and the cavitation number are the main factors affecting the onset of hole cavitation rather than the flow rate through the nozzle.

Hysteresis phenomena were also identified not only at the threshold cavitation number, but also at much higher CN values where flow transition was occurring within the injection holes. As it will be demonstrated in a following section, the flow in the holes converts from bubbly (incipient cavitation) to plug-type and then to fully separated until transient effects and cavitation originated in the sac volume become important. Not only the threshold cavitation number for transition was found to exhibit similar hysteresis effects, but also a time delay was observed between transition from one flow type to another under constant flow rate conditions. Although in large scale nozzles operating under steady-state conditions, such transient effects cannot be directly linked to the much shorter time scales in real size nozzles, it is expected that these phenomena may play a role in the development of cavitation in diesel engine injectors.

Location of cavitation initiation

As revealed in previous studies investigating nozzle cavitation, this phenomenon initiates in areas of low local pressure. Usually, these areas are found in the core of the recirculation zones formed at the upper corner of the injection holes when the needle is concentric and move towards the bottom corner for eccentric needle positions towards an injection hole [12]. Furthermore, in the case when the needle is positioned eccentric, off-center low-pressure regions are formed in holes being at an angle to the direction of the needle movement. These positions of low local pressure have been identified from CFD calculations (reported in [12]) in the same multi-hole nozzle examined here.

Nozzle discharge coefficient

One profound effect of hole cavitation is that it alters the nozzle discharge coefficient compared to that of the non-cavitating case; this is due to the blocking caused to the liquid flow by the presence of the cavitating structures. Since this affects the operating characteristics of the nozzle, this information is of significant importance to nozzle design and

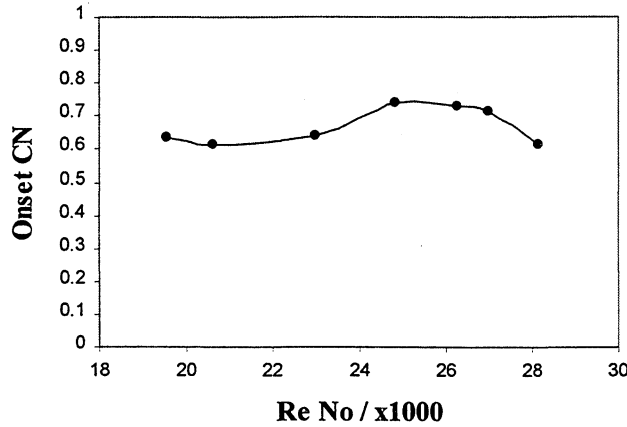


Figure 3 – Onset cavitation number as a function of Reynolds number

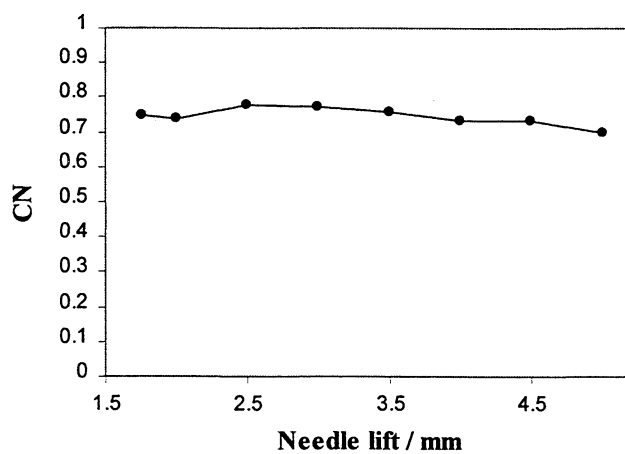


Figure 4 –Onset cavitation number as a function of needle lift

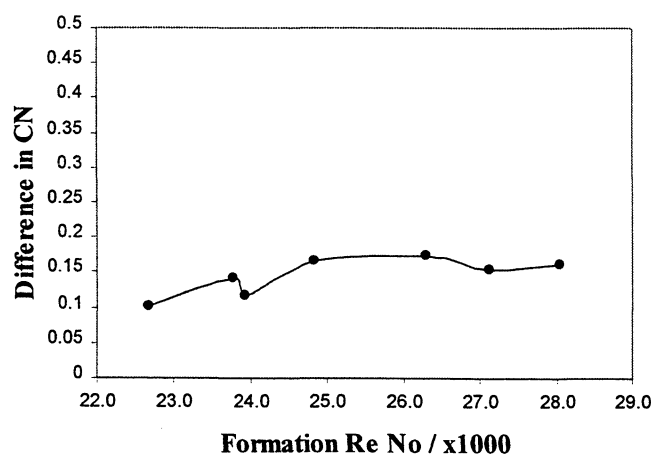


Figure 5 - Hysteresis on the cavitation number between onset and suppression of hole cavitation

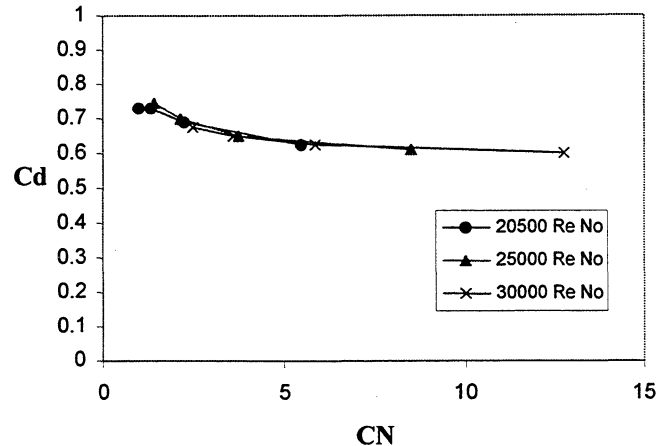


Figure 6 –Variation of nozzle discharge coefficient with cavitation number for different Reynolds numbers (needle lift=1.75 mm)

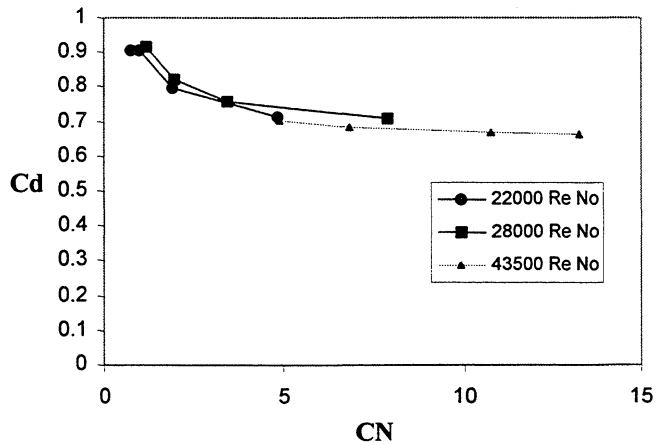


Figure 7 - Variation of nozzle discharge coefficient with cavitation number for different Reynolds numbers (needle lift=6 mm)

also to computational 1-D FIE models which require the discharge coefficient in order to predict accurately the fuel injection rate. Figure 6 and 7 show the variation of the nozzle discharge coefficient for two different needle lifts as a function of the cavitation number. In each graph, different curves have been plotted corresponding to different Reynolds numbers. The results confirm the findings of previous investigations reported in [18,31] that the nozzle discharge coefficient depends solely on the cavitation number rather than on the Reynolds number for the range of operating conditions of practical importance. Hence, effectively only one curve exists for the discharge coefficient of a specific nozzle geometry at a given lift independent of the Reynolds number. This trend seems to be the same for all needle lifts where at low CN the discharge coefficient coincides to that of the non-cavitating flow and decreases asymptotically to a minimum value at higher cavitation numbers.

Flow types

In the process of the present experiments two basic mechanisms of cavitation were identified. The first one is hole cavitation which initiates in the recirculation zones formed at the inlet of the injection holes, and the second one string-type cavitation which initiates in the sac volume. Although the nominal flow rate through the nozzle was kept constant at a specific operating point, the development of the cavitation structures was found to be transient, with certain phenomena taking place in time periods shorter than 100 μ s. As a consequence the images obtained vary, but those selected for presentation here are considered representative of the various cavitation regimes.

Independent of the position where cavitation bubbles first appearing, different flow regimes were identified to occur within the injection hole. As already mentioned, a bubbly flow regime has initially formed (incipient cavitation) which was gradually transformed into a film flow until complete flow separation within the recirculation zones took place. It was thus revealed that the cavitation number can be used as a macroscopic transition criterion from one flow type to another, where transition was found to be independent of the Reynolds number. Although the flow type was not influenced by the needle lift, the actual flow distribution was affected by the needle position as it will be revealed later. It should be pointed out, however, that the various threshold cavitation numbers at which flow transition was identified to occur, refer only to the specific nozzle design investigated here and cannot be used as a general criterion. Details about the various flow regimes identified in this project are presented below.

Bubbly flow (incipient cavitation)

Figure 9 shows typical images for this flow regime for two different cavitation numbers of 0.65 and 1.0 but keeping the Reynolds number constant, while Figure 10 shows a close-up obtained with the high magnification lens. Bubbly flow seems to be the first stage of cavitation, and is observed just after its onset. The range of CN where this pattern was evident was 0.65-1. It consists of small bubbles easily recognizable since the cloud is not very dense and their size seems to be relatively uniform. With increasing CN the density and thickness of the cloud also increases until it occupies about half the orifice diameter. A schematic representation of this type of flow is given in Figure 8. In addition, in this flow regime, a high frequency noise was produced after the onset of cavitation, which was different from the pre-film and film flow regimes described below.

Pre-film stage (plug-type cavitation)

With increasing CN the bubble clouds were becoming more opaque and it was not possible any more to distinguish between individual bubbles, until a dramatic change in the flow occurred at a cavitation number around 1.2. As the CN increase further, not only the liquid flowing through the top corner created a spatially wider recirculation zone, but also low pressure regions were formed at the hole sides due to the flow

entering through the space between two adjacent holes; thus, cavitation bubbles were formed at the sides of the hole. As the viewing direction of the obtained images was from the side of the hole, these bubbles seemed to generate a more dense bubble structure at the hole inlet. For small variations in the CN, the bubbles at the inlet were becoming larger than further downstream inside the hole and in some cases they collided giving rise to local cavitation films. Overall, the whole flow pattern started becoming relatively unstable since small changes in the flow rate were producing a vapor film.

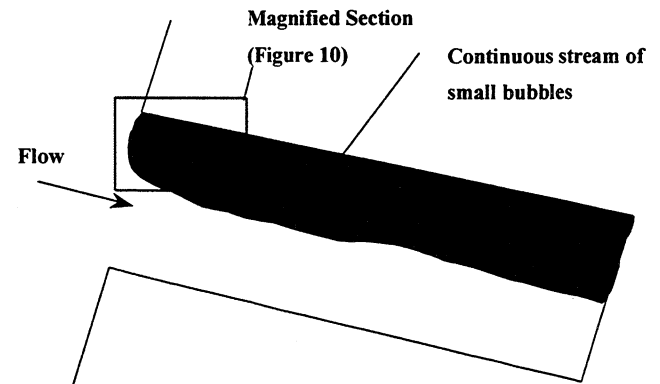


Figure 8 – Schematic representation of incipient cavitation flow regime

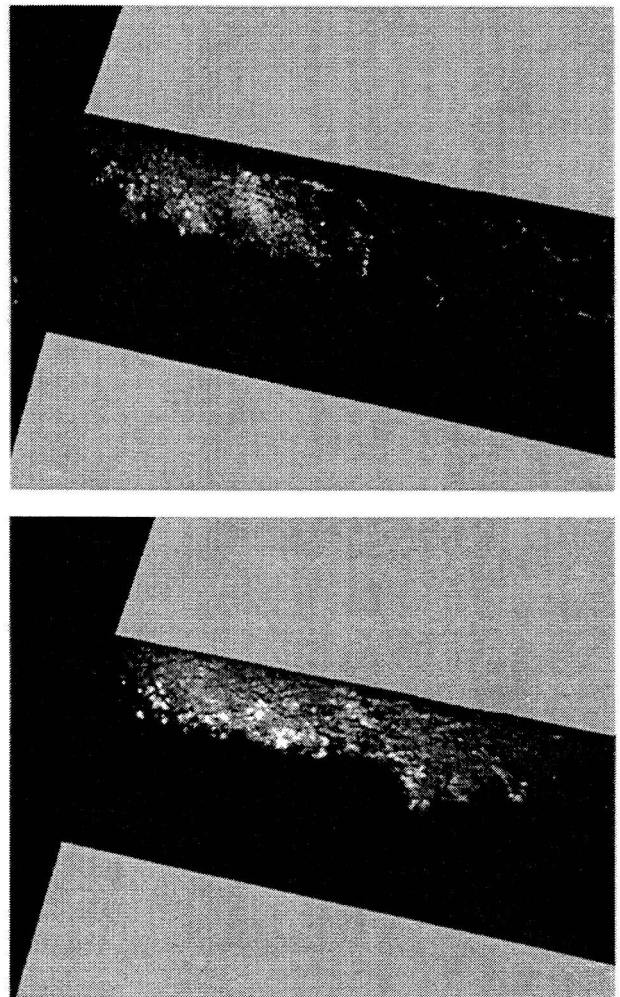


Figure 9 – Images of the incipient cavitation flow regime

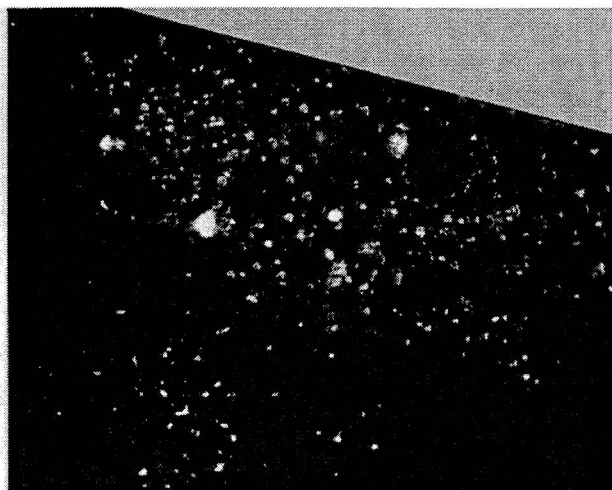


Figure 10 – Large magnification of incipient cavitation

The above flow regimes can be seen in Figure 12 while Figure 11 shows a schematic representation of the cavitation cloud; Figure 13 presents an image taken with the high magnification lens around the transition point from pre-film to a film cavitation pattern. Since these photographs cannot reveal the three-dimensional nature of the flow, a view taken from below the hole, shown schematically in Figure 14, was used to enhance the understanding about the cavitation pattern. The images shown in Figure 15 show that the cavitation bubbles occupy almost the whole width of the hole.

Film stage (separated flow)

Increasing the cavitation number above 1.3 resulted in a third transition stage where the bubbles were exploding at the separation zone forming a spatially continuous film of vapor that, in some instances, extended up to the hole exit. Typical images can be seen in Figure 17 taken for the same Reynolds and cavitation numbers, while Figure 18 shows a high magnification image within the recirculation zone at this flow regime. It is clear that complete flow separation occurs close to the hole inlet with ligaments formed at the sharp flow interface.

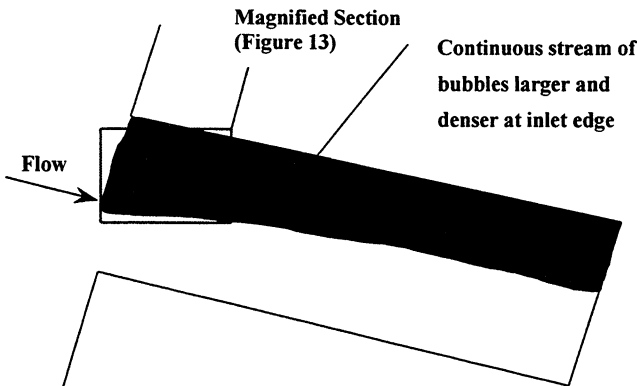


Figure 11 – Schematic representation of the pre-film stage flow regime

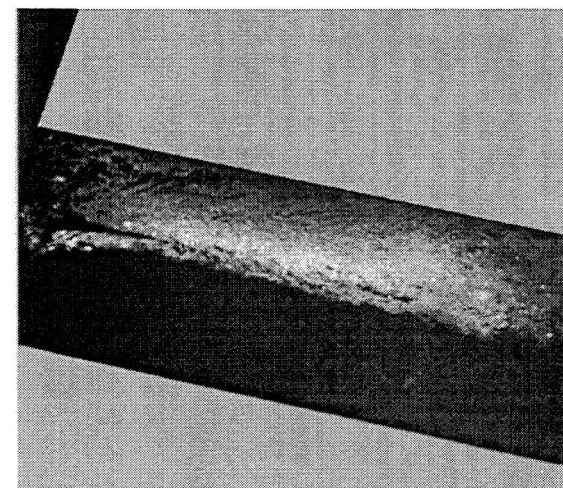
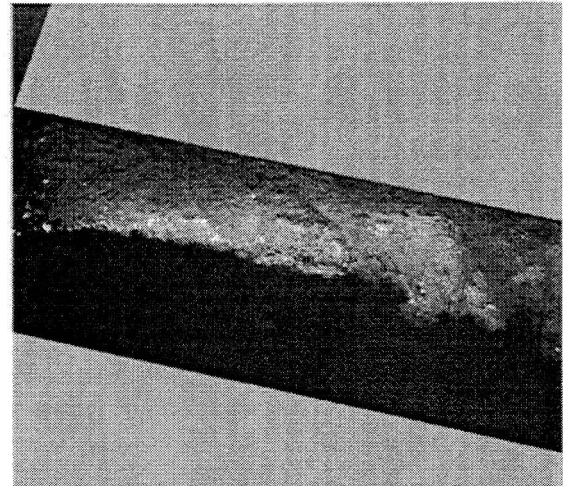


Figure 12 – Images of the pre-film stage flow regime

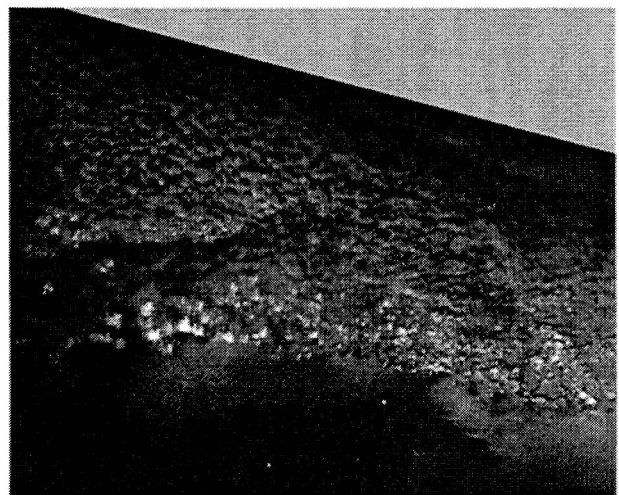


Figure 13 – Large magnification of the pre-film stage

This kind of flow shown schematically in Figure 16, is much more complex than the previous one and hence the view from below has proved essential for the understanding of the relevant phenomena.

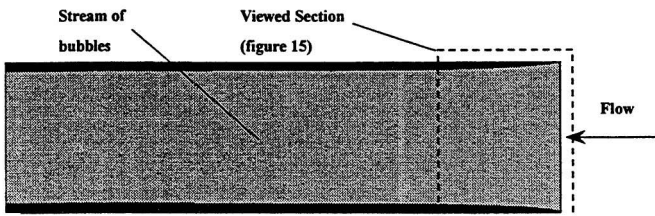


Figure 14 – Schematic representation of the pre-film stage flow regime as seen from below the injection hole

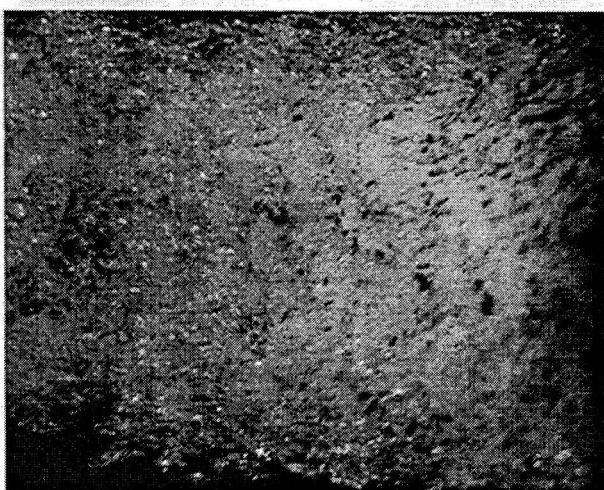
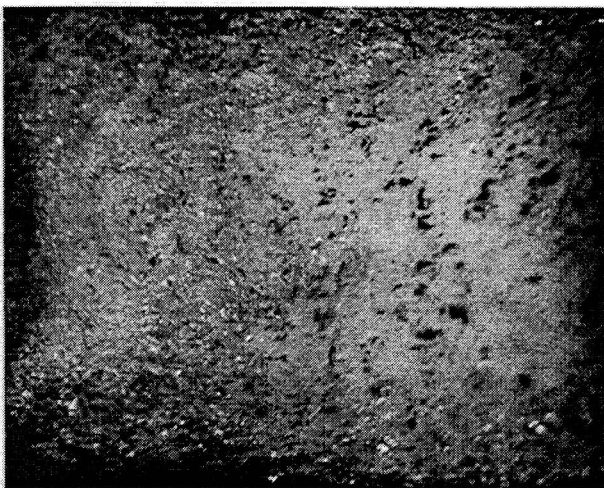


Figure 15 – Images of the pre-film stage flow regime as seen from below the injection hole

From this view, shown in Figure 20, it was deduced that the bright part of the image in the profile images of Figure 17 was a stream of emerging bubbles while the dark part represented the film. It seems that the film is relatively thin at the upper part of the hole (approximately 0.1 hole diameters) and follows the curved shape of the hole. A stream of bubbles was seen to emerge out of the film at downstream positions around the middle of the total hole length. Although the size of these bubbles was relatively large, it was not possible at this stage to make any quantitative estimation of their population and size. The bottom views also revealed that a separate cloud of

bubbles was originating at a point just after the entrance at both sides of the injection hole; once this cloud reached the stream of bubbles that were emerging out of the film, it became wider and eventually mixed with the film producing a more uniform bubbly flow towards the hole exit. However, at the hole inlet the film thickness was significantly greater than further downstream, covering more than a third of the hole diameter.

As it becomes clear from the above description, in this flow regime a number of different flow structures co-exist, varying from compact vapor films to ligaments developing on the interface areas and to stream of bubbles emerging from either the disruption of the film itself or from low pressure regions formed at the side of the injection holes.

By increasing further the CN up to the maximum values achievable with the existing experimental set-up, no drastic changes in the flow regime were observed. The film was maintaining the same shape but it was becoming more stable and smooth with increasing cavitation number and extended well outside the nozzle holes. When the maximum CN was attained, the fluid in the elastic hoses downstream of the transparent nozzle was in a white foam form. When running the injector at these conditions, it seemed useful to measure the pressure in the cavitation region. It was found that the pressure at the tapping of the brass fitting was almost vacuum while the pressure at the suction manifold was 0.4 bars. This implies that the pressure monitoring point has fallen in a separation zone where no liquid exists which is expected to be the case at the entrance to the hole. Hence it can be assumed that the pressure in the film was very close to vacuum.

As can be seen from Table 3, the actual Reynolds and cavitation numbers of a real injector correspond to film-type cavitation according to the above classification. Hence from now on most of the following results will refer to this flow condition since the other two flow regimes are expected to take place only at the very early or very late stages during the injection period.

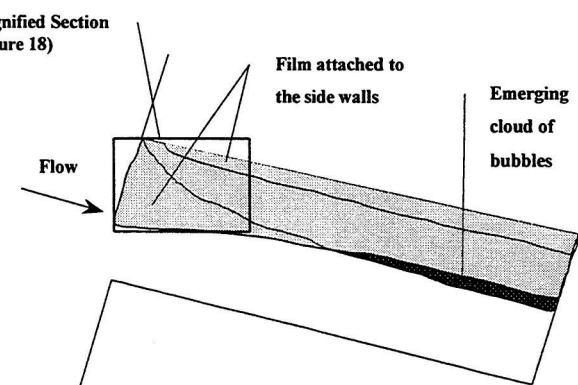


Figure 16 – Schematic representation of the film stage flow regime

Vortex formation

As already mentioned, a second type of cavitation structure was identified which originated well inside the sac volume in areas where the pressure is expected to be almost equal to the high upstream pressure and where no major separation or recirculation zones were identified in the CFD calculations.

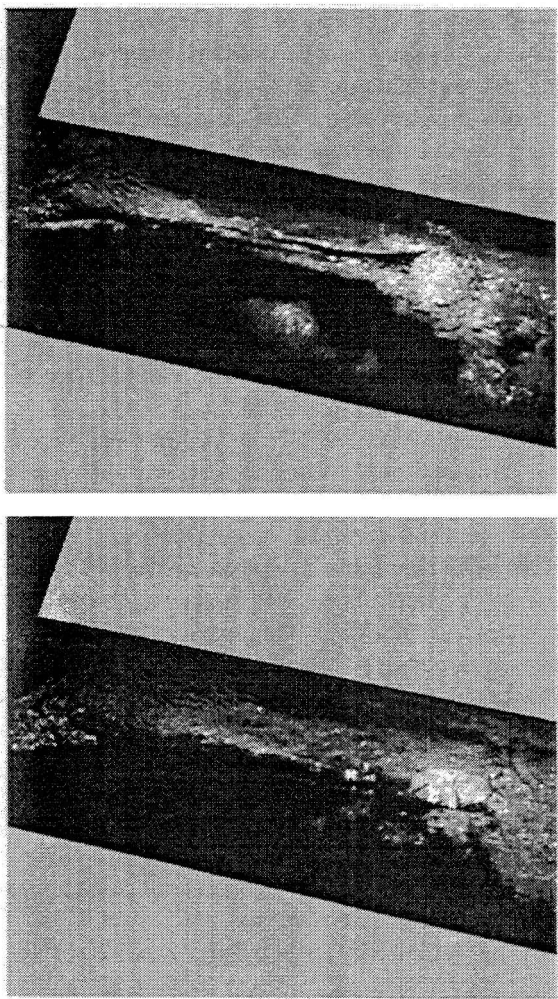


Figure 17 –Images of the film stage (separated) flow regime

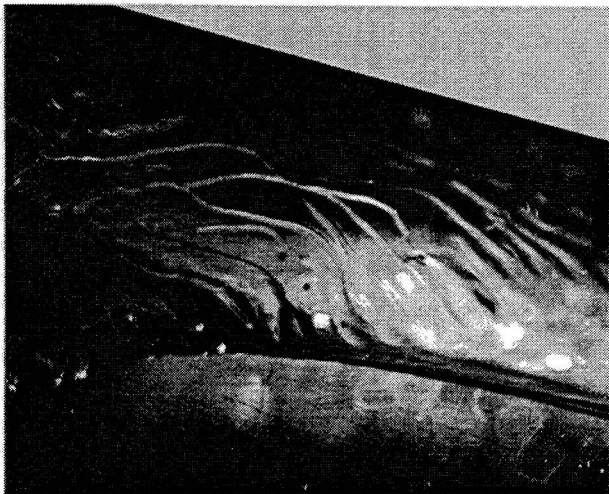


Figure 18 – Large magnification of the film stage (separated) flow regime

From a previous study [67], string cavitation was identified to be present in the sac volume of diesel injectors, which may explain the needle tip erosion observed in inclined production nozzles; this phenomenon, relatively unexplored up to now, has been usually attributed to ‘needle seat’ cavitation. The identified sac volume cavitation was in the form of bubble

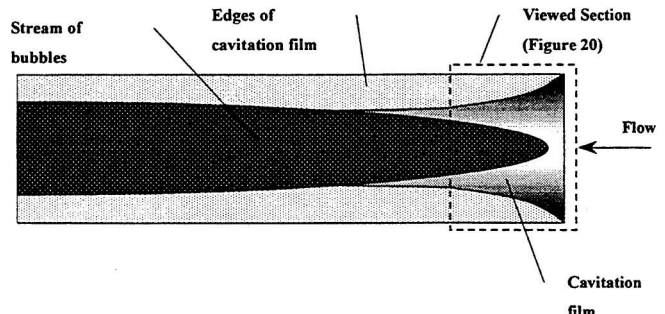


Figure 19 – Schematic representation of the film stage flow regime as seen from below the injection hole

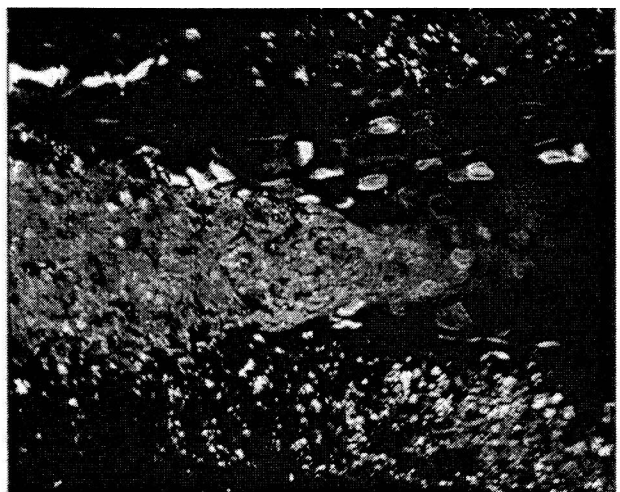


Figure 20 – Image of the film stage flow regime as seen from below the injection hole

streams forming a continuous string, which was extended to the region in between two adjacent holes. Figure 21 shows a typical image of this string pattern within the sac volume.

In order to identify the origins of the string type cavitation, a simple experiment aiming to visualize the sac volume flow was performed; a cloud of small air bubbles was inserted into the flow upstream of the transparent nozzle and was illuminated with a laser beam. Tracing of the movement of the bubbles revealed the instantaneous flow structure. A schematic representation of this flow is presented in Figures 22 and 23. Although the geometry of the examined nozzle is axisymmetric and no major convective flow has been predicted in the sac region [12], a cross flow was observed linking one side of the sac volume to the other while a vortex structure was identified to be present in the volume between adjacent holes. This was attributed to the interaction between the high momentum flow coming from upstream the nozzle and the cross flow, which occurred due to the intermittent ‘throttling’ of individual holes. As a result, the flow velocity at the vortex core leads to the formation of a low-pressure region and, subsequently, of cavitation bubbles. As the vortex enters the holes, it diffuses to a large conical cloud of bubbles, which can be seen at the lower part of the hole in Figure 21 and also schematically in Figure 23. In order to examine further the vortex formation in the sac volume, the needle was placed

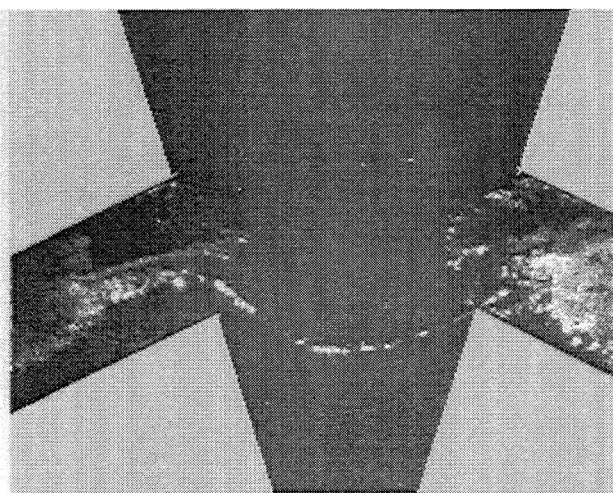


Figure 21 – Visualization of string cavitation inside the sac volume

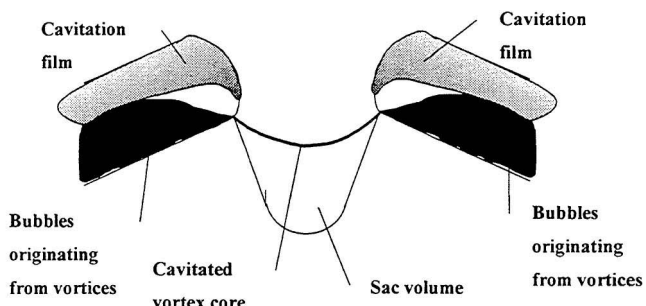


Figure 22 –Schematic representation of string-type cavitation inside the sac volume

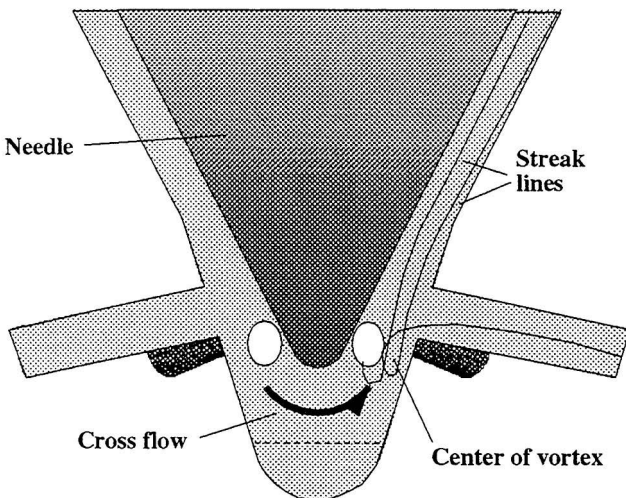


Figure 23 – Schematic representation of the flow inside the sac volume leading to the formation of string-type cavitation

eccentric towards an injection hole. Such needle displacement creates a strong convective motion within the sac volume along the plane of the needle movement under the needle tip and towards the hole located closer to the eccentric needle. It was found that the cavitation strings disappeared in these areas when a convective flow was present but were still

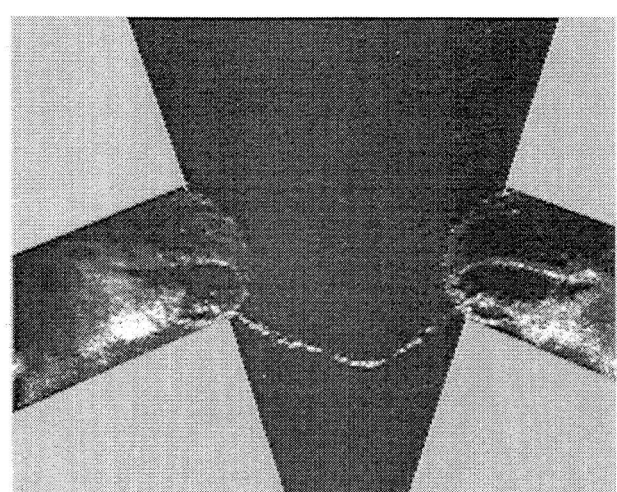
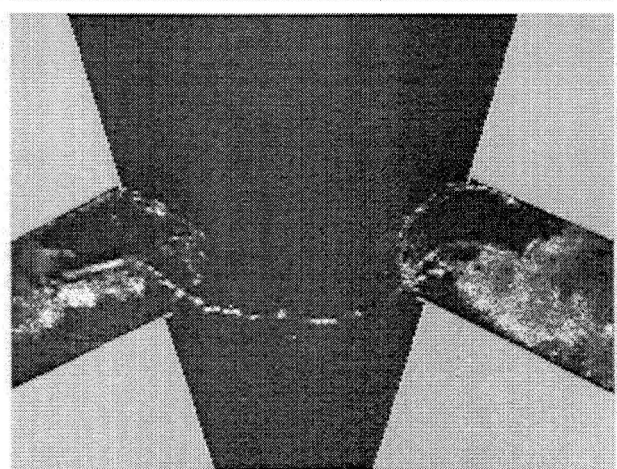
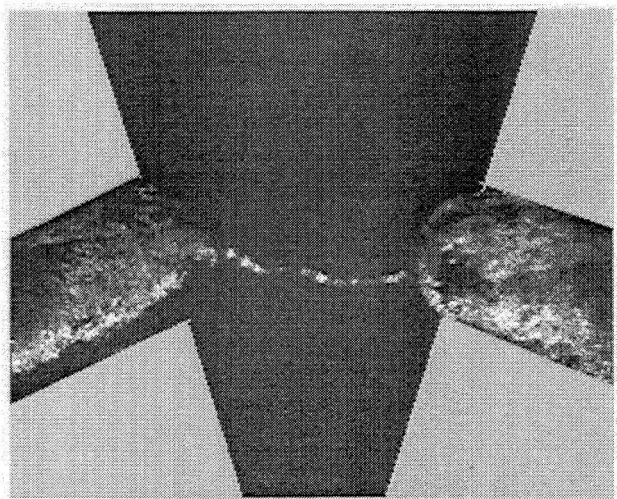


Figure 24 – Effect of the needle lift on the location of formation of string cavitation inside the sac volume (needle lift 1.75mm, 4 mm, 6 mm top to bottom)

present in the holes located at an angle relative to the direction of the needle movement. The axial position of these strings was found to depend strongly on the needle lift, as the images shown in Figure 24 reveal; in addition, their formation as well as their position, was found to be independent of the cavitation number. This time it is the Reynolds number, which is also a measure of the flow rate through the whole nozzle, that has an effect on the structure of these vortices; the cavitation

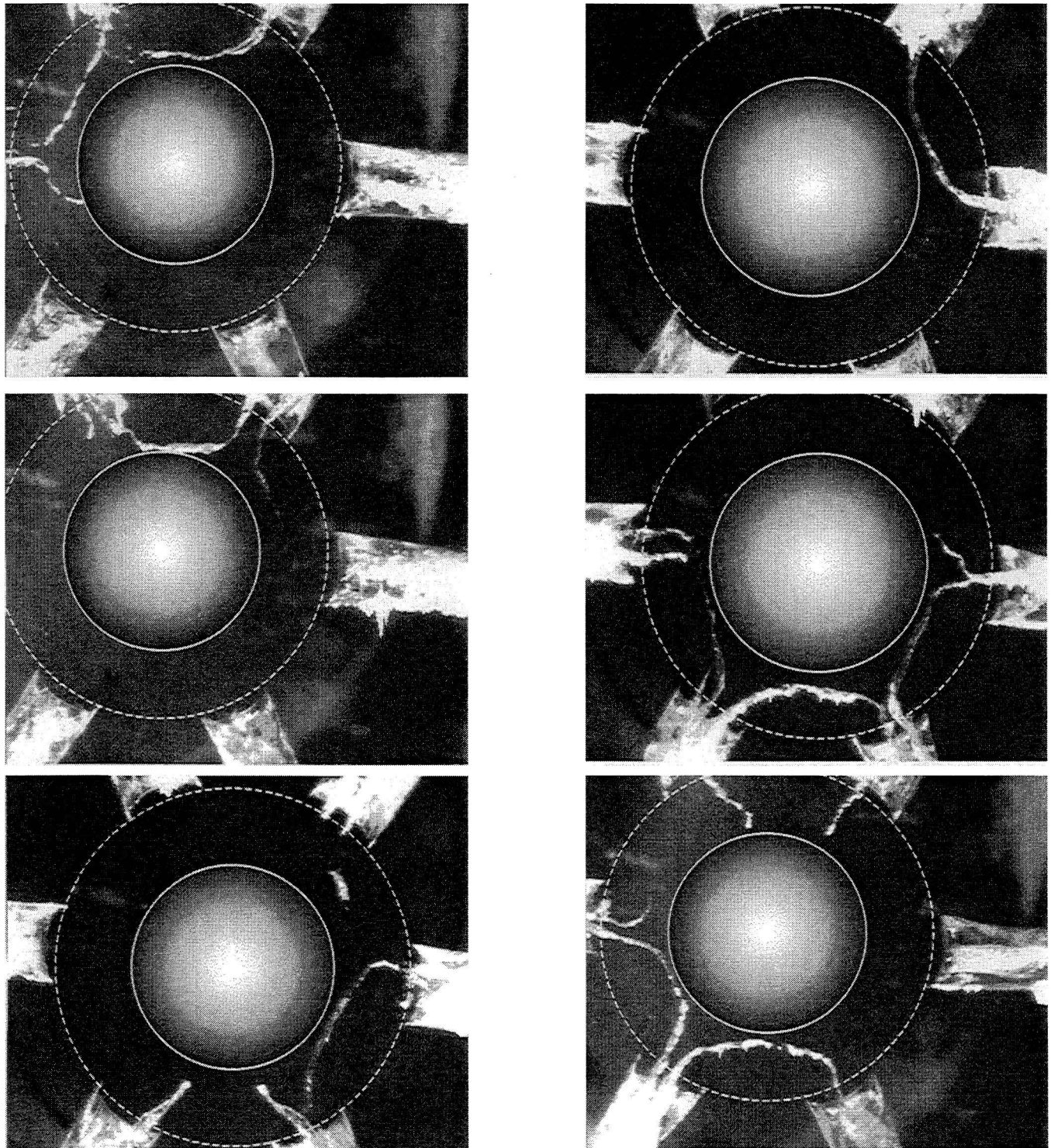


Figure 25 : Successive images of string cavitation at time intervals of $100 \mu\text{s}$; view from below the nozzle

strings were found to become more stable with increasing Reynolds number, implying that these phenomena depend on the velocity field inside the sac volume rather than on the pressure at the exit of the injection holes.

Another important feature of these cavitation strings was that their development took place in an extremely transient and intermittent way. To identify the time scales at which they were formed and travel, a successive set of images was taken

every $100 \mu\text{s}$ from below the nozzle; these images are presented in Figure 25. As can be seen, these strings appear and disappear within this small time interval and do not appear between all six holes simultaneously. The strings usually link adjacent holes in a random manner leading to rapid changes of the discharge coefficients of individual holes due to their significant size. This was indirectly confirmed from the large-scale flow motion identified within the sac volume. This

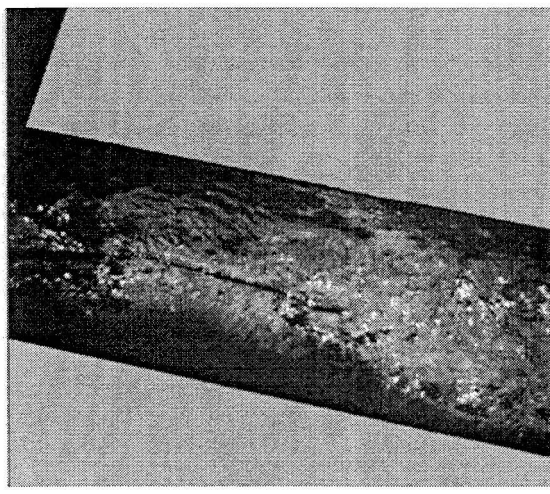
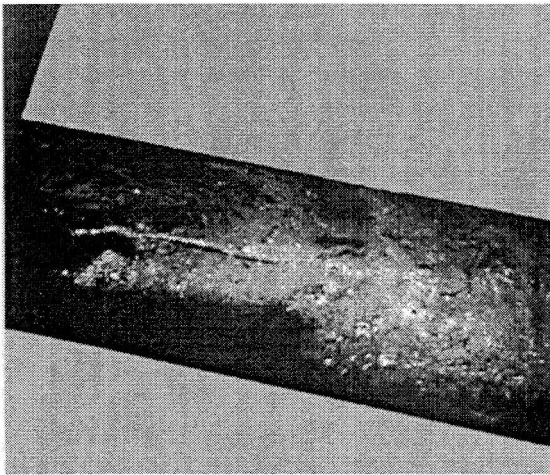


Figure 26–Interaction of pre-existing hole cavitation with string cavitation entering the hole. (100 μ s time interval)

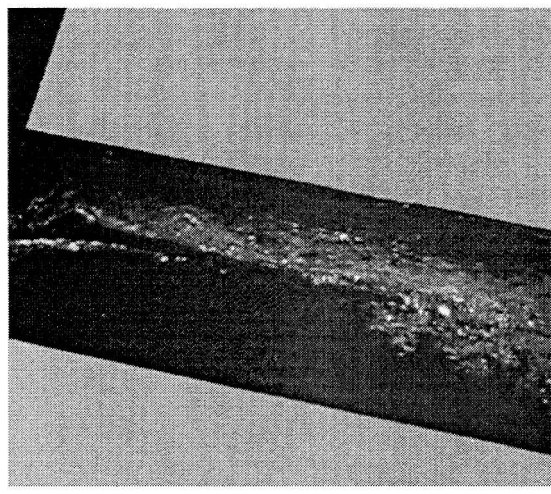
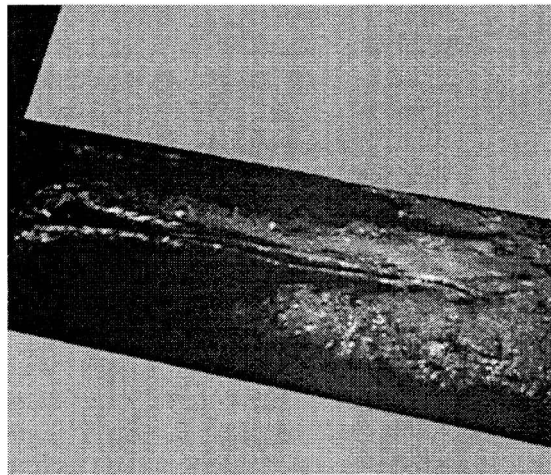


Figure 27– Interaction of pre-existing hole cavitation with string cavitation exiting the hole. (100 μ s time interval)

motion was easily seen from the tracing of the gas bubbles introduced into the model; it resembled a precessing periodic rotational motion with changing direction between adjacent holes.

For the extreme case of large needle eccentricities and small needle lifts, the vortices were so strong that they were covering the entire cross-sectional area of the hole while the whole cavitating pattern could be seen to exhibit a rotational motion. In such cases the discharge coefficient variations were so large that they could induce to the transparent model high frequency oscillations.

Effect of sac cavitation on hole flow

One of the most interesting findings of the present investigation is the interaction between the sac volume string and hole cavitation. Figures 26 and 27 show a representative sequence of events just after the entrance of a cavitating string into the hole. The transient development of this interaction can be seen by the difference between successive images taken at time intervals of 100 μ s. The large cloud of bubbles forming the string enters the hole from its lower part, it then expands possibly by the turbulent convection of the bubbles and interacts with the pre-existing cavitation films.

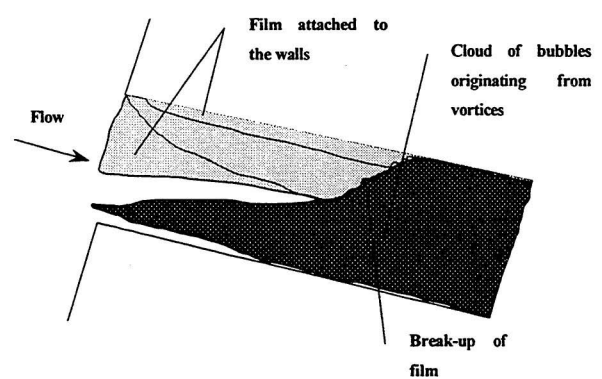


Figure 28 – Schematic representation of the effect of string cavitation on the hole flow

The result is the breaking of the film at a downstream location around the middle of the hole. As the images reveal, the hole flow after the film breakup becomes chaotic, and within a short time period it resembles a more uniform bubbly flow as shown schematically in Figure 28. However, due to the transient development of the strings in the sac volume, these phenomena are repeated in a periodic pattern giving rise to instantaneous variations in the hole discharge coefficient. One can easily

imagine that these flow instabilities should have a dominant effect on the atomization of the emerging spray and may be responsible for the spray-to-spray variations observed in diesel sprays injected from axisymmetric vertical nozzles (for example see [66]) and that incorporate guides to eliminate possible needle eccentricity effects; such variations are clearly not a geometric effect but rather the result of the nature of the flow itself in the sac volume and holes.

Effects of needle lift and eccentricity

The needle position inside the sac volume is one of the most important nozzle design factors affecting the flow pattern and the formation of the cavitation structures. Therefore, it was considered necessary to visualize the hole flow pattern for different values of needle lift and eccentricity. The latter, is generally believed to be the main factor responsible for the observed differences in the spray pattern generated from axisymmetric vertical nozzles [12]. As already mentioned, the eccentricity-induced asymmetry creates a flow through the sac volume from one side to another under the needle tip. According to [12] the pressure minimum in holes where the needle is eccentric towards them, tends to move from the upper

part of the entrance to the lower part. This is due to the fact that the needle is restricting the downward flow, making the upcoming flow from the sac region stronger and leading to flow separation in the lower part of the hole entrance. Furthermore, the cross flow in the sac volume due to the existing eccentricity enhances the vortex formations on the one side and suppresses them at the other. As a result, a drastically different cavitation pattern is observed in holes located towards the eccentric needle relative to those in the opposite side. Figures 29 and 30 show the flow pattern in the injection holes for different values of needle eccentricity. It is evident that the cavitation structure in the hole located closer to the needle is much more chaotic and bubbly due to the interaction of the cavitation zones formed at the bottom and top corners of the hole. However, in the hole located away from the needle, the flow is more stable with the film structures left unaffected by the needle movement. The effect of needle eccentricity on the hole flow is much more pronounced for small needle lifts where the turbulence is higher, the selective restriction of the passages by the needle more evident and the volume occupied by the needle in the sac greater. As expected, the needle lift proved to have a significant effect on the cavitation pattern. Although it was found that the cavitation number at onset was

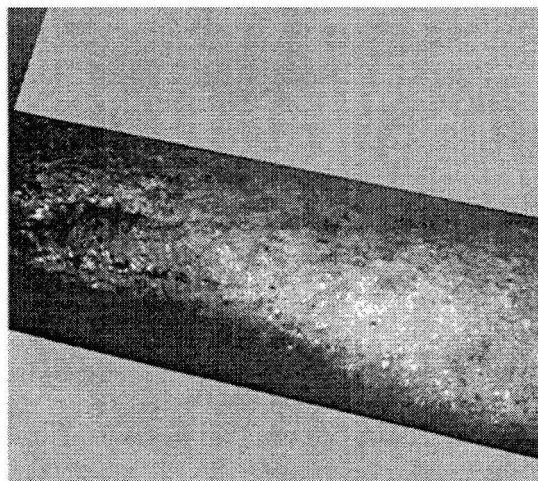
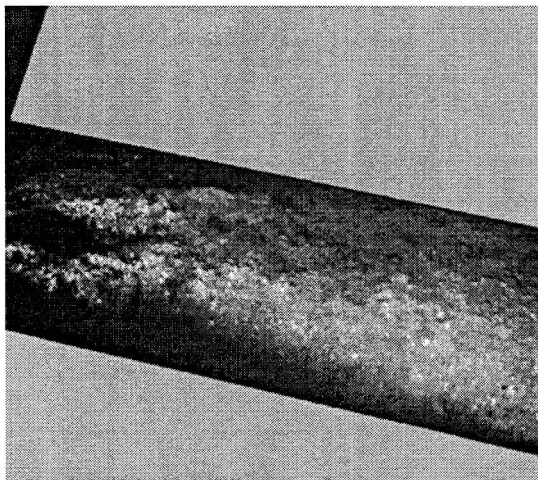


Figure 29 – Effect of needle eccentricity on hole cavitation (needle eccentric in the direction towards the injection hole)

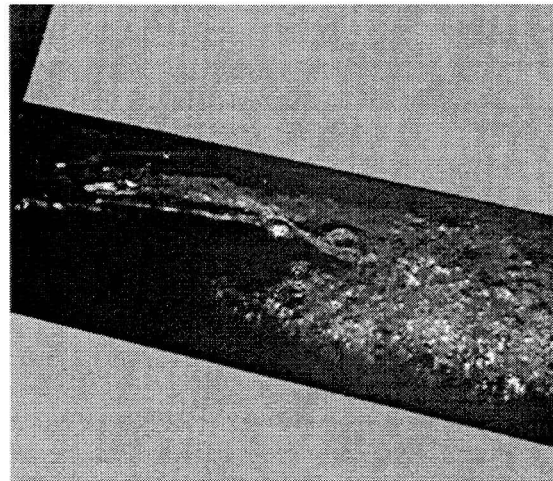
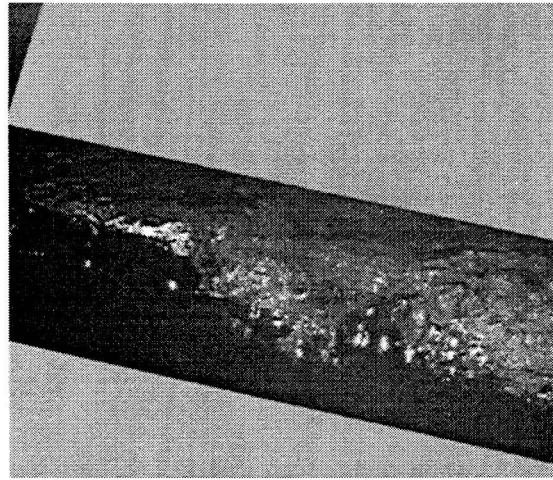


Figure 30 – Effect of needle eccentricity on hole cavitation (needle eccentric in the direction away from the injection hole)

unaffected by the needle lift, the resulting flow pattern was totally different. Figure 31 depicts flow images taken at the same Reynolds and cavitation numbers but for different needle lifts. The noticeable feature of these series of images is the shortening of the film length with decreasing needle lift. At the higher lift of 6mm, the film remains intact until the far end of the imaged area. The cavitation films were identified to be relatively stable while the cross sectional area covered by the

cavitation structures is about 35%. At the 4 mm lift the vortex effects at the lower side of the hole are more evident and frequently led to the progressive shortening of the film to about half of the hole length. Finally at the minimum lift of 1.75 mm almost no film can be seen as the turbulence has broken it up into small bubbles which seem to occupy the entire area of the hole.

CONCLUSIONS

A 20x enlarged transparent model of a six-hole vertical nozzle for 4-valve direct injection diesel engines was used in order to investigate the onset and development of cavitation in the sac volume and the injection holes. Simultaneous matching of Reynolds and cavitation numbers was achieved in order to simulate flow conditions similar to those in real-size nozzles; the corresponding Reynolds numbers were in the range 15,000-44,000 and the cavitation number in the range 0.65-15, while the needle lift was set to different values between 1.75 and 6.0 mm, which correspond to those at full lift of the first and second stages of two-spring injectors. The cavitating flow structures were visualized with a fast CCD camera equipped with high magnification lenses, which allowed details of the flow to be identified. Images of the cavitation flow were obtained both from the side and below the nozzle in order to reveal the three-dimensionality of the flow pattern.

The nozzle discharge coefficient varied with cavitation number and for a given needle lift it was independent of the Reynolds number. With increasing cavitation number, the nozzle discharge coefficient decreased asymptotically to a minimum value and different flow regimes were identified within the injection hole. Initially, a bubbly flow regime occurred (incipient cavitation) followed by pre-film stage cavitation. The last flow regime identified was the film type at which complete flow separation occurred within the injection hole. Although these flow types were not dependent on the Reynolds number or the actual needle position, the actual development of the cavitation structures was strongly affected by both the needle lift and the needle eccentricity. In addition to hole cavitation, cavitation strings were observed to form inside the sac volume. These strings seemed to develop transiently and periodically between adjacent holes. As they were convected inside the injection holes, they interacted with pre-existing cavitation films giving rise to significant disturbances of the flow and hole-to-hole variations.

Overall, the most general conclusion from this work is that variations in the flow pattern between holes do exist even in axisymmetric vertical multi-hole nozzles and are due not only to geometric effects such as needle eccentricity, but also to the complex two-phase flow present in the sac volume and holes after the onset of cavitation.

ACKNOWLEDGEMENTS

The authors would like to thank Ford Motor Company for financial support and to acknowledge the contribution of Mr. R. Godwin of Pulse Photonics Ltd. to the development of the cavitation imaging system.

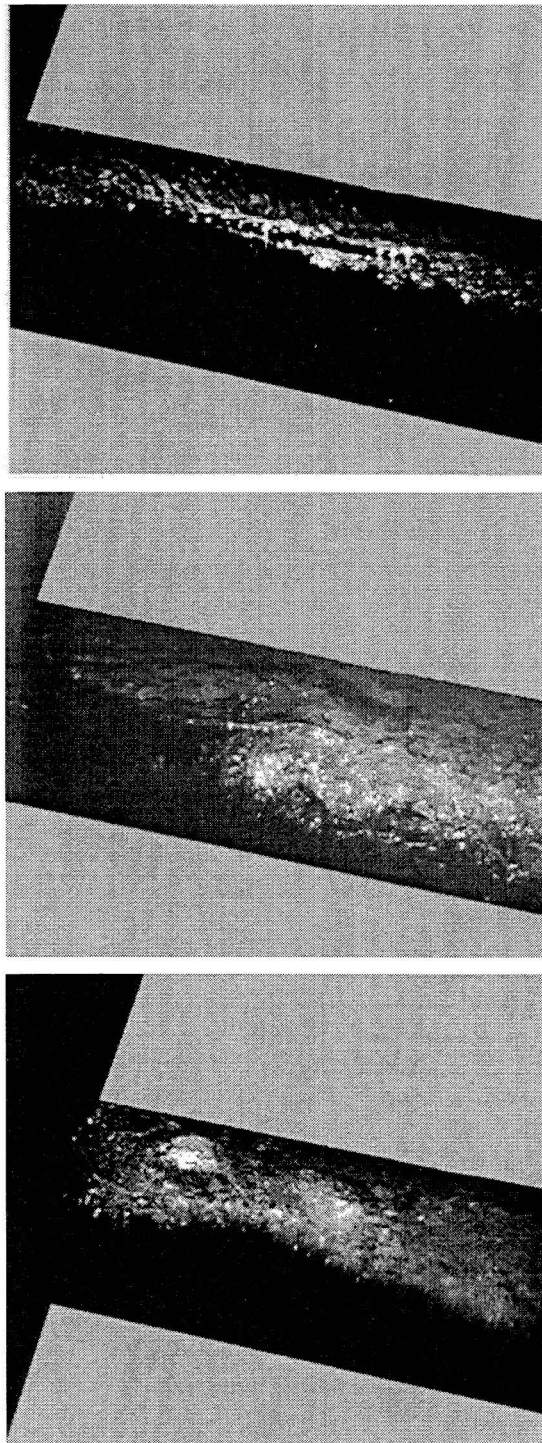


Figure 31 – Effect of needle lift on hole cavitation for same Reynolds and cavitation numbers (needle lift 6mm, 4mm, 1.75mm from top to bottom)

Authors	Ref	Nozzle type	Scale-up factor	Reynolds number	Cavitation number	Refractive Index	Measurement
Arcoumanis et al.	[11]	Single-hole	7	20,000	-	Yes	LDV in the nozzle gallery
Arcoumanis et al.	[12]	6-hole, Vertical mini-sac	20	20,000	-	Yes	LDV in the sac volume and the injection holes Visualisation of hole cavitation
Date et al.	[13]	4-hole, Inclined	40	64,000	-	No	Velocity from particle trace images Pressure distribution
Hiroyasu et	[14]	Single-hole Step with various inlet shapes	10	30,000	-	No	Visualisation of hole cavitation
Kato et al.	[15]	4-hole, inclined mini-sac	40	65,000	-	No	Pressure distribution
Kim et al.	[16]	2-hole Vertical & inclined Sac, mini sac & VCO	10	40,000	-	No	Visualisation of hole cavitation
Knox-Kelecy and Farrel	[17]	Single-hole step	50	10,500	-	No	PDPA-turbulence characteristics
Soteriou et al.	[18]	Single-hole, sac type Vertical & inclined 5-hole Vertical & inclined sac & VCO	20	5,000-30,000	0.4-50	No	Visualisation of hole cavitation
Soteriou et al.	[20]	Single-hole step	20	10,000	0.5-15	Yes	LDV in the hole Visualisation of the hole cavitation
He & Ruiz	[3]	Single-hole	200	13.800	-	No	LDV in the hole, turbulence characteristics

Table 1 – Experimental investigations on large-scale transparent nozzles

Authors	Ref	Hole size (mm)	Maximum injection pressure (bar)
Badock et al.	[21,25]	0.24	600
Dan et al.	[22]	0.18-0.40	200
Chaves et al.	[23,24]	0.20	500
Bergwerk	[23,24]	0.30	100

Table 2 - Experimental investigations on real size single-hole transparent nozzles

Reynolds number	15,000	44,000
Equivalent flow rate in real-size nozzle	15 mm ³ /ms	45 mm ³ /ms
Range of pressures	1.2-5.2 bar	
Range of mean injection velocities	10-20 m/s	
Maximum cavitation number	15	
Vapor pressure of Tetralin at 30°C	0.008 - 0.012 bar	
Vapor pressure of Turpentine at 30°C	0.1 bar	
Equivalent injection pressure in real-size nozzle (back pressure 40 bar)	600 bar	

Table 3 - Range of Reynolds and cavitation numbers simulated in the large-scale nozzle

REFERENCES

- 1.Boehner W. and Hummel K. "Common rail injection system for commercial Diesel vehicles", SAE Paper 970345, 1997.
- 2.Guerrasi N. and Dupraz P. "A common rail injection system for high speed direct injection Diesel engines", SAE Paper 980803, 1998.
- 3.He L. and Ruiz F. "Effect of cavitation on flow and turbulence in plain orifices for high speed atomization", Atomization and Sprays, vol. 5, pp. 569-584, 1995.
- 4.Tamaki N., Shimizu M., Nishida K. and Hiroyasu H. "Effects of cavitation and internal flow on atomization of a liquid jet", Atomization and Sprays, vol.8, pp. 179-197, 1998.
- 5.Zhen H., Yiming S., Shiga S., Nakamura H., Karasawa T. "The orifice flow pattern, pressure characteristics, and their effects on the atomization of fuel containing dissolved gas", Atomization and Sprays, vol. 4, pp. 123-133, 1994.
- 6.Park B.S. and Lee S.Y. "An experimental investigation of the flash atomization mechanism", Atomization and sprays, vol. 4, pp. 159-179, 1994.
- 7.Santangelo P.J. and Sojka P.E. "A holographic investigation of the near - nozzle structure of an effervescent atomizer - produced spray", Atomization and sprays, Vol. 5, pp. 137-155, 1995.
8. Arcoumanis C. and Gavaises M. "Linking nozzle flow with spray characteristics in a diesel fuel injection system", Atomisation and Sprays, vol. 8, pp. 307-347, 1998
9. Arcoumanis C., Gavaises M. and French V. "Effect of fuel injection processes on the structure of Diesel sprays, SAE Paper 970799, 1997.
10. Chaves H., Bode J., Hentschel W., Kubitzek A., Obermeier F., Schindler K.P., Schneider T. "Fuel spray in Diesel engines Part I: spray formation", Proceedings of the 3rd Int. Conf. Innovation and Reliability in Automotive Design and Testing, paper 2.6.2, 1995.
11. Arcoumanis C., Nouri J.M. and Andrews R.J. "Application of refractive index matching to a diesel nozzle internal flow", Proc. IMechE Seminar on Diesel Fuel Injection Systems, April 14-15, 1992.
12. Arcoumanis C., Gavaises M. Nouri J.M., Wahab E. and Horrocks R. , "Analysis of the flow in the nozzle of a vertical multi-hole Diesel engine injector", SAE Paper 980811, 1998.
13. Date K., Nobechi H., Kano H., Kato M., and Oya T. "Experimental analysis of fuel flow characteristics in the nozzle for direct injection engines", SAE Paper 931002, 1993.
- 14.Hiroyasu H., Arai M. and Shimizu M. "Break-up length of a liquid jet and internal flow in a nozzle" ICCLASS-91 Gaithersburg, MD, U.S.A. July 1991.
15. Kato M., Kano H., Date K., Oya T. and Niizuma K."Flow analysis in nozzle hole in consideration of cavitation", SAE Paper 970052, 1997.
16. Kim J-H., Nishida K., Yoshizaki T. and Hiroyasu H. "Characterization of flows in the sac chamber and the discharge hole of a DI Diesel injection nozzle by using a transparent model nozzle" SAE Paper 972942, 1997.
17. Knox-Kelecy A.L. and Farrell P.V. "Spectral characteristics of turbulent flow in a ccale model of a Diesel fuel injector nozzle", SAE Paper 930924, 1993.
18. Soteriou C.C.E., Andrews R.J., and Smith M. "Direct injection Diesel sprays and the effect of cavitation and hydraulic flip on atomization", SAE Paper 950080, 1995.
- 19.Yule A.J., Dalli A.M. and Yeong K.B. "Transient cavitation and separation in a scaled-up model of a VCO orifice", ILASS Conf., July 6-8, Manchester U.K., 1998
20. Soteriou C., Smith M., Andrews R. "Diesel injection - laser light sheet illumination of the development of cavitation in orifices", IMechE C529/018/98, 1998
21. Badock C., Wirth R., Kampmann S. and Tropea C. "Fundamental Study of the Influence of cavitation on the internal flow and atomization of Diesel sprays", ILASS Conf., July 8-10, Florence, 1997
22. Dan T., Yamamoto T., Senda J. and Fujimoto H. "Effect of nozzle configuration for characteristics of non-reacting Diesel fuel spray", SAE Paper 970355, 1997
- 23.Chaves H., Knapp M., Kubitzek A., Obermeier F., and Schneider T. "Experimental study of cavitation in the nozzle hole of Diesel injectors using transparent nozzles", SAE Paper 950290, 1995
24. Chaves H. and Obermeier F. "Correlation between light absorption signals of cavitating nozzle flow within and outside of the hole of a transparent diesel injection nozzle", ILASS Conf., July 6-8, Manchester U.K., 1998
25. Badoch H., Wirth R., Fath A. and Leipertz A. "Application of laser light sheet technique for the investigation of cavitation phenomena in real size diesel injection nozzles", ILASS Conf., July 6-8, Manchester U.K., 1998
- 26.Trevena D.H. Cavitation & tension in liquids, Adam Hilger Ltd., 1987
27. Knapp R.T., Daily J.W., Hammit F.G. Cavitation, McGraw Hill Book Company, 1970
- 28.Minami K. and Shoham O. "Transient two-phase flow behaviour in pipelines - experiment and modeling", Int. J. Multiphase Flow, Vol. 20, No. 4, pp. 739-752, 1994
- 29.Dominick J. and Durst F. "Measurement of bubble size, velocity and concentration in flashing flow behind a sudden constriction", Int. J. Multiphase Flow, Vol. 21, No 6, pp. 1047-1062, 1995
30. Okajima M., Kato M., Kano H., Tojo S., and Katagiri M. "Contribution of optimum nozzle design to injection rate control", SAE Paper 910185, 1991
- 31.Bergwerk W. "Flow pattern in diesel nozzle spray holes", Proc. Instn. Mech Engrs, Vol 173, No 25, pp 655-674, 1959
32. Ohrn T.R., Senser D.W., and Lefebvre A.H. "Geometrical effects on discharge coefficients for plain - orifice atomizers", Atomization and Sprays, vol. 1, no. 2, pp. 137-153, 1991
33. Spikes R.H. and Pennington G.A. "Discharge coefficient of small submerged orifices", Proc. Inst. Mech. Eng., Vol 173, No 25, pp 661-674, 1959
- 34.Abraham F.F. Homogeneous nucleation theory, Academic Press, 1974
35. Brennen C.E. Cavitation and bubble dynamics, Oxford University Press, 1995
36. Carey V.P., Liquid-vapor phase-change phenomena, Hemishre Publishing Corporation, 1992
37. Hsu Y-Y. and Graham R.W. Transport processes in boiling and two-phase systems, Hemisphere puplishing corporation, 1976

38. Stralen S. and Cole R. Boiling phenomena, Hemisphere Publishing Corporation, 1979
39. Carpenedo L., Cluti P. and Iernetti G. "Cavitation nuclei distribution in liquids by tensile strength measurements", Acoustics Letters, Vol. 7, No. 4, pp. 50-55, 1983
40. Finkelstein Y. and Tamir A. "Formation of gas bubbles in supersaturated solutions of gases in water", AIChE J. Vol. 31, No 9, pp. 1409-1419, 1985
41. Hentschel W., Zarschizky H. and Lauterborn W. "Recording and automatical analysis of pulsed off-axis holograms for determination of cavitation nuclei size spectra", Optics Communications, Vol. 53, No 2, pp. 69-73, 1985
42. Neppiras E.A. and Nolting B.E. "Cavitation produced by ultrasonics : Theoretical conditions for the onset of cavitation", Proc. Phys. Soc., Vol 64, 12-B, pp. 1032-1038, 1951
43. Nolting B.E. and Neppiras E.A. "Cavitation produced by ultrasonics", Proc. Phys. Soc., Vol 63 9-B, pp. 674-685, 1950
44. Al-Hayes R.A.M. and Winterton R.H.S. "Bubble diameter on detachment in flowing liquids" Int. J. Heat Mass Transfer, Vol. 24, pp.223-230, 1981
45. Kenning D.B.R. and Del Valle V.H.M. "Fully developed nucleate boiling: overlap of areas of influence and interference between bubble sites", Int. J. Heat Mass Transfer, Vol. 24, No 6, pp. 1025-1032, 1981
46. Mei R., Chen W. and Klausner J. "Vapor bubble growth in heterogeneous boiling - I. Growth rate and thermal effects", Int. J. Heat Mass Transfer, Vol. 38, No 5, pp. 921-934, 1995
47. Mei R., Chen W. and Klausner J. "Vapor bubble growth in heterogeneous boiling - I. Formulation", Int. J. Heat Mass Transfer, Vol. 38, No 5, pp. 909-919, 1995
48. Yang S.R. and Kim R.H."A mathematical model of the pool boiling nucleation site density in terms of the surface characteristics", Int. J. Heat Mass Transfer, Vol. 31, No 4, pp. 1127-1135, 1988
49. Duraiswami R. and Chahine G.L. "Analytical study of a gas bubble in the flow field of a line vortex", FED-Vol. 135, pp. 69-76, Cavitation and Multiphase Flow Forum, ASME 1992
50. Lush P.A. "Cavity dynamics in a duct flow", C191/83@IMechE, 1983
51. Nigmatulin R.I., Khabeev N.S. and Nagiev F.B. "Dynamics, heat and mass transfer of vapor-gas bubbles in a liquid", Int. J. Heat Mass Transfer, Vol. 24, No. 6, pp. 1033-1044, 1981
52. Plesset M.S. "The dynamics of cavitation bubbles", J. Applied Mechanics, pp. 277-282, 1949
53. Plesset M.S. and Prosperetti A. "Bubble dynamics and cavitation", Ann. Rev. Fluid Mech, Vol. 9, pp. 145-185, 1977
54. Young F.R. Cavitation, McGraw Hill Book Company, 1989
55. Feng Z.C. and Leal L.G. "Nonlinear bubble dynamics", Ann. Rev. Fluid Mech., Vol. 29, pp. 201-243, 1997
56. Boulton-Stone J.M. and Blake J.R. "Gas bubbles bursting at a free surface", JMF, Vol. 254, pp. 437-466, 1993
57. Fujikawa S. and Akamatsu T. "Effects of non-equilibrium condensation of vapour on the pressure wave produced by the collapse of a bubble in a liquid", JFM, Vol. 97, part 3, pp. 481-512, 1980
58. D'Agostino L. and Brennen C. "Linearized dynamics of spherical bubble clouds", JFM, Vol. 199, pp. 155-176, 1989
59. Rubinstein J. "Bubble interaction effects on waves in bubbly liquids", J. Acoust. Soc. Am. Vol 77, No 6, pp. 2061-2066, 1985
60. Takahira H., Akamatsu T. and Fujikawa S. "Some analytical aspects on the dynamics of a cluster of bubbles", IMechE C453/016, pp. 9-15, 1992
61. Sadhal S.S., Ayyaswamy P.S. and Chung J.N. Transport phenomena with drops and bubbles, Springer-Verlag New York Inc., 1997
62. Clift R., Grace J.R., Weber M.E. Bubbles droplets and particles, Academic Press, Inc., 1978
63. Nigmatulin R.I. Dynamics of multiphase media, Revised and Augmented ed., Vol. 1, Hemisphere Publishing Corporation, New York, 1991. Originally published by Nauka Moscow under the title : Dinamika Mnogofaznykh Sred
64. Collier J.G. and Thome J. Convective boiling and condensation, Oxford University Press, 1997
65. Whalley P.B. Boiling condensation and gas-liquid flow, Clarendon Press, Oxford, 1987
66. Ming-Chia Lai Wang T-C., Xie X., Han J-S., Henein N., Schwarz E. and Bryzik W. "Microscopic characterization of diesel sprays at VCO nozzle exit", SAE Paper 982542, 1998
67. Kim J.H., Nishida K. and Hiroyasu H. "Characteristics of the internal flow in a diesel injection nozzle", ICLASS 97, Seoul, 1997